

Artificially evolved *Synechococcus* PCC6301 Rubisco variants exhibit improvements in folding and catalytic efficiency

Dina N. GREENE*¹, Spencer M. WHITNEY†¹ and Ichiro MATSUMURA*²

*Department of Biochemistry, Center for Fundamental and Applied Molecular Evolution, Emory University School of Medicine, Rollins Research Center, Atlanta, GA 30322, U.S.A., and †Molecular Plant Physiology, Research School of Biological Sciences, The Australian National University, Canberra ACT 0200, Australia

The photosynthetic CO₂-fixing enzyme, Rubisco (ribulose-1,5-bisphosphate carboxylase/oxygenase), is responsible for most of the world's biomass, but is a slow non-specific catalyst. We seek to identify and overcome the chemical and biological constraints that limit the evolutionary potential of Rubisco in Nature. Recently, the horizontal transfer of Calvin cycle genes (*rbcL*, *rbcS* and *prkA*) from cyanobacteria (*Synechococcus* PCC6301) to γ -proteobacteria (*Escherichia coli*) was emulated in the laboratory. Three unique Rubisco variants containing single (M259T) and double (M259T/A8S, M259T/F342S) amino acid substitutions in the L (large) subunit were identified after three rounds of random mutagenesis and selection in *E. coli*. Here we show that the M259T mutation did not increase steady-state levels of *rbcL* mRNA or L protein. It instead improved the yield of properly folded L subunit in *E. coli* 4–9-fold by decreasing its natural propensity to misfold *in vivo* and/or by enhancing its interaction

with the GroES–GroEL chaperonins. The addition of osmolites to the growth media enhanced productive folding of the M259T L subunit relative to the wild-type L subunit, while overexpression of the trigger factor and DnaK/DnaJ/GrpE chaperones impeded Rubisco assembly. The evolved enzymes showed improvement in their kinetic properties with the M259T variant showing a 12% increase in carboxylation turnover rate (k_{cat}^c), a 15% improvement in its K_M for CO₂ and no change in its K_M for ribulose-1,5-bisphosphate or its CO₂/O₂ selectivity. The results of the present study show that the directed evolution of the *Synechococcus* Rubisco in *E. coli* can elicit improvements in folding and catalytic efficiency.

Key words: CO₂ fixation, directed evolution, metabolic engineering, protein engineering, ribulose-1,5-bisphosphate carboxylase/oxygenase (Rubisco).

INTRODUCTION

Rubisco (ribulose-1,5-bisphosphate carboxylase/oxygenase) catalyses the nucleophilic carboxylation of ribulose-P₂ (D-ribulose-1,5-bisphosphate). This conversion of inorganic CO₂ into carbohydrate is frequently the rate-limiting step in the synthesis of most of the world's biomass [1]. In spite of its biological importance, Rubisco is an inefficient catalyst, particularly at limiting CO₂ concentrations. Its turnover rate is less than one-thousandth of many other plant enzymes [2]. Moreover, the efficiency of Rubisco-catalysed carbon assimilation is further compromised by the fixation of O₂, which competes with CO₂ for addition to ribulose-P₂. The 2-phosphoglycolate product of the oxygenation reaction is recycled by photorespiration, an energy consuming process that releases one-quarter of the incorporated carbon [3]. It is not clear why such an important enzyme is so slow and non-specific. Our goals are to understand the physical, chemical and biological constraints to the adaptive evolution of Rubisco, and to find ways to overcome them.

Natural selection generally favours enzyme variants that evince speed (high turnover, k_{cat}), high substrate affinity (low Michaelis constant, K_M) and high substrate specificity (k_{cat}/K_M primary substrate divided by k_{cat}/K_M secondary substrate). Extant Rubisco homologues from different photosynthetic organisms show significant variation in all three parameters (see [4] for a summary). Their K_M in reactions with CO₂ as the substrate (K_c) varies from 3–340 μ M and the corresponding carboxylation turn-over rates

(k_{cat}^c) vary between 1 and 13 s⁻¹. The ability of Rubiscos to discriminate CO₂ from O₂, defined as its specificity factor ($S_{c/o}$), varies between 10 and 240. $S_{c/o}$ is determined by dividing a Rubisco's carboxylation efficiency (k_{cat}^c/K_c) by its oxygenation efficiency (k_{cat}^o/K_o), where k_{cat}^o is the O₂ saturated oxygenation rate and K_o is the K_M for O₂ [5]. This natural variability in Rubisco kinetics has encouraged attempts to engineer kinetically improved versions of the enzyme [1,6,7].

Phylogenetic analyses can highlight patterns that reflect horizontal gene transfer or gene duplication and selective loss [8,9]. For example, phylogenetic analyses of Rubisco L (large) subunit genes (*rbcL*) suggest that this gene was horizontally transferred at least four times during the evolution of proteobacteria, cyanobacteria and plastids [10]. Although natural mechanisms that effect the transfer of DNA between genomes have been identified [11], the mechanisms of gene adaptation upon transfer to new cellular micro-environments remain poorly understood. Gene sequence comparisons can sometimes identify instances of molecular adaptation, although most beneficial mutations are obscured by the accumulation of functionally neutral mutations [12]. The 'resurrection' and *in vitro* characterization of ancestral proteins can offer unambiguous evidence for molecular adaptation, but only if the investigator can correctly predict the biochemical tests to conduct [13]. Directed evolution experiments can emulate hypothetical evolutionary events, thereby 'resurrecting' ancestral proteins and the conditions in which they were selected.

Abbreviations used: 2-carboxyarabinitol-P₂, 2'-carboxyarabinitol-1,5-bisphosphate; carboxypentitol-P₂, isomeric mixture of carboxyarabinitol-P₂ and 2'-carboxyarabinitol-1,5-bisphosphate; fructose-P₂, fructose-1,6-bisphosphate; IPTG, isopropyl β -D-thiogalactoside; KJE, DnaK/DnaJ/GrpE; L, large; LB-kan, Luria-Bertani medium containing 50 μ g/ml kanamycin; *prkA*, phosphoribulokinase; ribulose-P₂, D-ribulose-1,5-bisphosphate; Rubisco, ribulose-P₂ carboxylase/oxygenase; TF, 50 kDa trigger factor chaperone.

¹ These authors contributed equally to this work.

² To whom correspondence should be addressed (email imatsum@emory.edu).

Table 1 Features of the *Synechococcus* PCC6301 Rubisco genes and proteins used in the present studyWT, wild-type *rbcL-rbcS* operon.

Rubisco name	<i>rbcLS</i> mutant allele number*	Silent <i>rbcL</i> mutations
(-)WT	–	nil
Revertant WT	–	c489t, c783t, t799c
(-)M259T	–	nil
M259T	2.29	c489t, c783t, t799c
A8S/M259T	2.24	c783t, t799c
M259T/F342S	3.54	t702c, c783t, t799c

* Clone number described in [16].

In the present study, we investigated the horizontal transfer and subsequent adaptation of cyanobacteria (*Synechococcus* PCC-6301) Rubisco to a new cellular environment by imitating the process in the laboratory. Although the hexadecameric *Synechococcus* Rubisco structurally resembles Rubisco in all higher plants [comprising eight L and eight S (small) subunits; L₈S₈] it is unique in its ability to be functionally expressed in *E. coli* [14,15]. By simultaneously transferring the *Synechococcus* *prkA* (phosphoribulokinase), *rbcL* and *rbcS* (coding the Rubisco small subunit) genes into wild-type *E. coli* strain K-12 we have developed a high throughput genetic selection system to study the adaptive mechanism(s) that improves the fitness of Rubisco in this non-natural host. The selection pressure in the system is the alleviation of ribulose-P₂ toxicity (produced by phosphorylation of ribulose-5-phosphate by PRK) via its oxygenation or carboxylation by Rubisco [16]. Three unique Rubisco variants (M259T, M259T/A8S and M259T/F342S; Table 1) emerged after three rounds of random mutagenesis and genetic selection, all sharing the M259T mutation. Preliminary biochemical studies showed that *E. coli* cells expressing the evolved Rubiscos exhibited 2–5-fold more carboxylase activity than those expressing the wild-type enzyme. Purified C-terminal-His₆-tagged versions of these mutant proteins showed similar increases in specific activity [16]. Here we extend these initial observations to examine how the mutations in the horizontally transferred *Synechococcus* PCC6301 *rbcL* increased the fitness of the host *E. coli* cell during selection.

EXPERIMENTAL PROCEDURES

Materials

The construction of the *rbcLS*-pET30a+ expression vectors containing the wild-type *Synechococcus* PCC6301 Rubisco *rbcL-rbcS* operon and those encoding the single (M259T) and double (M259T/A8S, M259T/F342S) amino acid mutations (with and without C-terminal His₆ tags fused to the large subunit; Table 1), and most of the materials used for the present study have been described previously [16]. The Sephadex® G-50 Fine and the radiolabelled NaH¹⁴CO₃ were from Pharmacia (GE Healthcare). The 0.2 micron nylon filters were from Alltech. All other chemicals were from Sigma Chemicals.

Site-directed mutagenesis

PCR-mediated site-directed mutagenesis was applied to change Thr²⁵⁹ of Rubisco 2.29 back to a methionine residue (to create an otherwise wild-type *rbcLS* with only silent mutations), and to

introduce the M259T (t776c) mutation into the wild-type *rbcLS* gene [to create the (-)M259T Rubisco without silent mutations].

Expression of wild-type and artificially evolved Rubiscos

E. coli BL21(DE3) cells were transformed with the *rbcLS*-pET30a+ plasmids encoding the wild-type and mutant Rubisco variants. The transformed cells were grown separately at 23 °C to mid-logarithmic phase in LB-kan (Luria–Bertani medium containing 50 µg/ml kanamycin) and Rubisco expression was induced for 16 h with 0.5 mM IPTG (isopropyl β-D-thiogalactoside). The cells were harvested by centrifugation (5 min at 5000 g at 4 °C), resuspended in extraction buffer (100 mM Hepps/NaOH, pH 8.0, 1 mM EDTA, 2 mM dithiothreitol and 0.05 % *E. coli* protease inhibitor cocktail) and lysed by passage through a French pressure cell (140 MPa). A 50 µl aliquot of lysate (total cellular protein) was removed for SDS/PAGE analysis and the remainder centrifuged at 38 000 g for 10 min at 4 °C to remove the insoluble material. Aliquots of the supernatant were either assayed for protein content (1 µl), Rubisco content (100 µl; see below) or processed for SDS/PAGE (12 % gels) and non-denaturing PAGE (4–12 % acrylamide gradient) analysis as described previously [17].

Measuring Rubisco content by [¹⁴C]2-carboxyarabinitol-P₂ (2'-carboxyarabinitol-1,5-bisphosphate) binding

The concentration of Rubisco active sites was determined by the stoichiometric binding of the inhibitor [¹⁴C]2-carboxyarabinitol-P₂. Ribulose-P₂ was synthesized and purified as described previously [18] and used to make ¹⁴C-labelled carboxypentitol-P₂ (97 000 cpm/nmol) according to the method used by Pierce et al. [19]. Carboxypentitol-P₂ is an isometric mixture of carboxyribitol-P₂ and carboxyarabinitol-P₂. The latter is a transition-state analogue that binds preferentially to activated Rubisco in an almost irreversible manner [20]. Samples containing Rubisco were activated with 25 mM NaHCO₃ and 20 mM MgCl₂ at 25 °C for 30 min before incubating with 27 µM [¹⁴C]2-carboxypentitol-P₂ for 15–45 min. The Rubisco–[¹⁴C]2-carboxyarabinitol-P₂ complex was separated from unbound [¹⁴C]2-carboxypentitol-P₂ by size-exclusion chromatography and Rubisco content calculated as described previously [21].

Purification of native (untagged) Rubisco variants

The Rubisco variants were expressed in 1 litre cultures of *E. coli* *rbcLS*-pET30/BL21(DE3) cells as described above. After 16 h of induction with 0.5 mM IPTG, the cells were harvested by centrifugation (5 min at 6000 g at 4 °C), resuspended in 45 ml ice-cold extraction buffer, and lysed with a French pressure cell. The cellular debris was removed by centrifugation at 35 000 g for 15 min at 4 °C. The Rubiscos were purified by heating the extracts at 50 °C, followed by precipitation with ammonium sulfate, and then ion-exchange chromatography using a Mono-Q (10/10) column (GE Healthcare) as described previously [22]. Collected fractions (5 ml) were assayed for substrate-saturated ribulose-P₂ carboxylase activity using NaH¹⁴CO₃ (2 Ci/mol; GE Healthcare) [23]. Appropriate fractions were pooled and a saturated ammonium sulfate solution (pH 7) was slowly added to 60 % (w/v) final concentration. The Rubisco precipitate was collected by centrifugation at 22 000 g for 15 min at 4 °C, dissolved in 3 ml storage buffer (15 mM Hepps/NaOH, pH 8.0, 1 mM EDTA and 50 mM NaCl) and then dialysed using a Slide-a-lyzer cassette (Pierce Chemical Co.) against 1 litre of storage buffer overnight at 4 °C. The dialysis was repeated against fresh storage buffer for 2–4 h and then against storage buffer containing

20% (v/v) glycerol for 4 h. The purified Rubisco was frozen in liquid nitrogen and stored at -70°C . SDS/PAGE and non-denaturing PAGE analysis showed that these preparations were $> 95\%$ pure.

Kinetic assays

The purified Rubisco preparations were used to measure the CO_2/O_2 specificity ($S_{c/o}$) at pH 8.3 as described previously [24]. $S_{c/o}$ was measured in reactions equilibrated with an atmosphere of O_2 accurately mixed with 0.1% (v/v) CO_2 using Wostoff pumps. The Michaelis constants for substrates CO_2 (K_c) and ribulose- P_2 (K_{RuBP}) were measured in ^{14}C -fixation assays at 25°C and pH 8, according to the method described previously [23]. The purified enzyme was pre-incubated at 25°C for 30 min in buffer containing 20 mM MgCl_2 and 25 mM NaHCO_3 , and K_c measurements were performed in nitrogen-sparged septum-capped scintillation vials. The reactions were initiated by the addition of 10 μl of purified enzyme to 1 ml of N_2 -equilibrated assay buffer (100 mM Hepes/NaOH, pH 8, 20 mM MgCl_2 , 0.8 mM ribulose- P_2 and 0.1 mg/ml carbonic anhydrase) containing various concentrations of $\text{NaH}^{14}\text{CO}_3$. K_{RuBP} measurements were performed in air-equilibrated assay buffer containing different concentrations of ribulose- P_2 (0–2 mM). The ^{14}C -assays were stopped after 1.5 or 2 min with 0.5 vol. of 25% (v/v) formic acid and dried at 80°C . The residue was dissolved in 0.5 ml of water before the addition of 1 ml of scintillant (UltimaGold XR; Perkin Elmer Life Sciences) for scintillation counting. The Michaelis constants were determined by fitting the data to the Michaelis–Menten equation. From the K_c measurements, the catalytic turnover rate (k^{cat}) was calculated by dividing the extrapolated maximal carboxylase activity by the concentration of Rubisco active sites in the assay (measured by ^{14}C -2-carboxyarabinitol- P_2 binding, as described above).

PAGE and immunoblot analyses of protein expression in wild-type and artificially evolved Rubiscos

SDS/PAGE, non-denaturing PAGE and immunoblot analyses were performed according to methods described previously [17]. Immunoblot analyses using polyclonal antisera raised in rabbits against purified *Synechococcus* PCC6301 Rubisco or tobacco Rubisco were performed.

Reverse transcriptase–real time PCR

E. coli strain DH5 Δlac (DE3) [25] was separately transformed with the *rbcLS*-pET30a+ plasmids coding for wild-type and M259T Rubisco. The transformed cells were propagated to mid-logarithmic stage in LB-kan. Rubisco expression was induced with 0.5 mM IPTG overnight at 23°C . Total RNA was extracted using the RNeasy kit (Qiagen) and its concentration determined by absorbance measurements at 260 nm using a Shimadzu UV-1601 spectrophotometer. The RNA (30 or 0.3 ng) and various amounts of the *rbcLS*-pET30a+ plasmids were used in conjunction with the iScript one-step real time PCR kit (Bio-Rad) using the *rbcL*-specific primer 5'-TGGTGACCGACCCTTCTTC-3' (reverse) to synthesize cDNA. Real time PCR reactions were performed in duplicate using *rbcL*-specific reverse and forward (5'-GCTGACCGACATGGATCGGTACAA-3') primers according to manufacturer's instructions. Melt curve analysis confirmed the stability, accuracy and specificity of the primer pair. The PCR amplification reactions were monitored with an iCycler real time PCR machine (Bio-Rad) and the amount of *rbcL* mRNA in each sample quantified using the accompanying software.

Analysis of wild-type and M259T Rubisco expression with the addition of osmolites and chaperones

E. coli BL21(DE3) cells were transformed with pET30a+ (negative control) or the *rbcLS*-pET30a+ plasmids (encoding either the wild-type or M259T Rubisco). The cells were grown in LB-kan in the presence or absence of 0.3 M NaCl and 20 mM proline at 37°C to a D_{600} of 0.8 before the induction of Rubisco expression with 0.5 mM IPTG at 23°C for 5 h. Each cell type was separately co-transformed with plasmids pGro7 (encoding GroEL/ES), pKJE7 (encoding DnaJ/DnaK/GrpE), or pTF16 (encoding the trigger factor) (a set of chaperone expression vectors have been described previously [26,27]) and similarly grown in LB-kan containing chloramphenicol (30 $\mu\text{g}/\text{ml}$). Protein expression was similarly induced at 23°C for 5 h with 0.5 mM IPTG (Rubisco), 0.05% (w/v) L-arabinose (pGro7, pKJE7, pTF16 and pG-KJE8) or/and 5 $\mu\text{g}/\text{ml}$ tetracycline (pG-KJE8 and pG-Tf2). Measurement of Rubisco content by SDS/PAGE, non-denaturing PAGE and ^{14}C -carboxyarabinitol- P_2 binding was standardized relative to cell density by measurement of the D_{600} immediately prior to harvesting 15 ml of the cells by centrifugation (5 min at 4000 g). For BL21(DE3) cells transformed with pET30 or *rbcLS*-pET30 a D_{600} of 1.0 was equivalent to 2.7×10^8 cells/ml.

CD spectra analyses

Far UV spectra and thermal denaturation were measured using a Jasco-810 spectropolarimeter. Far UV spectra were measured at 20°C between 185 and 260 nm in 0.5 nm increments using a 0.01-cm path-length cell, a 2 nm bandwidth, a 4 s response time and a scanning speed of 20 nm/min. Thermal denaturation (unfolding) curves were measured at 2°C increments at a rate of $1^{\circ}\text{C}/\text{min}$ between 20 and 80°C in a 0.1-cm path-length cell at 222 nm.

RESULTS

Our objective was to elucidate the biochemical mechanism(s) by which the *Synechococcus* PCC6301 Rubisco adapted to our *E. coli*-based selection system (Table 1). Previous analyses indicated that compared with wild-type controls the artificially evolved Rubisco variants were expressed 2–5-fold more efficiently in *E. coli* and the specific carboxylase activities of purified His₆-tagged enzymes were approx. 5-fold greater [16]. In the present study, we have carefully characterized the steady-state kinetics of the native (not tagged) versions of the wild-type and evolved Rubisco variants, and examine the mechanisms that account for the expression differences.

Catalytic properties

The untagged wild-type *Synechococcus* PCC6301 Rubisco and the M259T, A8S/M259T and M259T/F342S variant enzymes were purified from recombinant *E. coli* by ammonium sulfate fractionation and ion exchange chromatography. Affinity tag-fusions at either the N- or C-terminus of the Rubisco L subunit were avoided since modifications to these regions can influence the enzymes kinetics [28,29]. The CO_2/O_2 specificity ($S_{c/o}$), the Michaelis constants of the Rubisco/substrate interactions (K_c , K_M for CO_2 ; K_{RuBP} , K_M for ribulose- P_2), and the substrate saturated carboxylation rate (k^{cat}) of the wild-type PCC6301 Rubisco were similar to values reported previously (Table 2). The replicate $S_{c/o}$ measurements were highly reproducible and revealed no change for the M259T enzyme and modest decreases ($< 15\%$) for the A8S/M259T and M259T/F342S Rubisco variants.

The M259T variant evinced a 12% increase in k^{cat} , while the A8S/M259T and M259T/F342S double mutants exhibited

Table 2 Kinetic properties of purified wild-type and mutant *Synechococcus* PCC6301 Rubiscos identified by genetic selection

WT, wild-type.

Rubisco type	S_{C/O_2} , CO ₂ /O ₂ specificity*	k_{cat}^{c} carboxylation turnover rate (s ⁻¹)	K_c Michaelis constant for CO ₂ (μM)	k_{cat}^c/K_c Carboxylation efficiency (M ⁻¹ · s ⁻¹)	K_{RUBP} Michaelis constant for pure ribulose-P ₂ (μM)
WT <i>rbcL-rbcS</i> operon	43.9 ± 1.8	11.4 ± 0.1*	273 ± 10*	4.2 × 10 ⁴	63.9 ± 4.5*
	43.0 ± 1.0†	11.6†	284†	4.1 × 10 ⁴ †	54 ± 3‡
M259T	42.8 ± 3.9	12.8 ± 0.2*	237 ± 10*	5.4 × 10 ⁴	67.0 ± 3.2*
A8S/M259T	40.5 ± 2.6	11.4 ± 0.1§	216 ± 9§	5.3 × 10 ⁴	47.8 ± 4.6§
M259T/F342S	38.4 ± 0.7	10.0 ± 0.1§	207 ± 8§	4.8 × 10 ⁴	33.7 ± 5.9§

* Means ± S.D. for measurements made in triplicate.

† Kinetic parameters as in [22].

‡ Kinetic parameters as in [17].

§ Value from single measurement with error derived from Michaelis–Menten hyperbolic curve fit.

slightly diminished k_{cat}^c values (wild-type-like and 12 % less than wild-type respectively). The K_c for the M259T, A8S/M259T and M259T/F342S Rubisco reactions were 13 %, 21 % and 24 % lower than the comparable wild-type value respectively. Likewise, K_{RUBP} values of the A8S/M259T and M259T/F342S enzyme-catalysed reactions were reduced 25 % and 47 % respectively, while the K_{RUBP} for M259T remained comparatively unchanged. The three evolved Rubiscos exhibited 15–28 % improvements in carboxylation efficiency (k_{cat}^c/K_c) relative to the wild-type enzyme (Table 2).

Rubisco synthesis and assembly in *E. coli*

To examine whether the mutations in the evolved Rubisco variants influenced their production in *E. coli*, the total and soluble cellular proteins were analysed by SDS/PAGE. For the six Rubisco variants examined, the L band was the predominant protein in the total cellular protein samples (Figure 1A). To more accurately assess the relative amounts of the L subunit expressed, each sample was diluted 100-fold and re-analysed by SDS/PAGE (Figure 1B). We observed little difference in the amount of L subunit synthesized, apart from a modest (<2-fold) increase in the amount of total L in the *E. coli* expressing the A8S/M259T Rubisco. Likewise, the nucleotide substitutions did not influence the steady state *rbcL* mRNA levels. Reverse transcriptase–real time PCR measurements revealed similar amounts of *rbcL* message in cells expressing the wild-type or M259T enzyme (Table 1); both alleles showed an approx. 10-fold increase in the amount of *rbcL* mRNA upon induction with IPTG (results not shown). These results showed that the nucleotide substitutions in *rbcL* (non-silent mutations, and the c783t and t799c silent mutations) had little, if any, influence on the transcriptional or translational processing of the gene variants.

SDS/PAGE analysis of comparable soluble cellular protein samples showed that >90 % of the L subunits were insoluble (Figure 1C). Immunodetection indicated that the relative levels of soluble L and S subunits were higher in cell extracts containing evolved Rubisco variants than in control extracts containing the wild-type protein (Figure 1D). These 2–4-fold differences in the amount of soluble L correlated with the different concentrations of functional L₈S₈ Rubisco measured by carboxy-arabinitol-binding (Figure 1E) and non-denaturing PAGE (Figure 1F). They are consistent with previous findings that most, if not all, of the soluble L subunit detected in *E. coli* extracts assembled into functional L₈S₈ enzyme [17,30]. In contrast, the production of the S subunit in *E. coli* does not limit assembly of PCC6301 Rubisco, since as much as 50 % of the soluble S subunit is not assembled in L₈S₈ complexes, but can readily do

so when supplied with L₈ cores [31]. Taken together, these data suggested the M259T mutation present in the L subunit of all three artificially evolved Rubisco variants improves the ability of the L subunit to fold and/or assemble correctly with the S subunit into the functional enzyme within *E. coli*. Notably the additional F342S mutation compromised the yield of functional Rubisco produced by approx. 2-fold, consistent with previous results [16].

E. coli chaperone-assisted folding

We examined whether the improved folding and assembly of the M259T L in *E. coli* resulted from an increased compatibility between the mutated L subunits and several key *E. coli* chaperone complexes. Indeed, 10-fold improvements in the amount of cyanobacterial Rubisco folded correctly and assembled in *E. coli* can be obtained by overexpressing the GroES/GroEL chaperonins [14,32]. The 70 kDa chaperone DnaK that works in concert with its co-chaperones DnaJ (a chaperone activating protein) and GrpE (a nucleotide exchange factor) is also requisite for productive folding of bacterial Rubiscos in *E. coli* [15]. The 50-kDa TF (trigger factor) chaperone similarly co-translationally binds nascent peptide chains to prevent their misfolding and aggregation [27,33]. *E. coli* BL21(DE3) cells expressing the wild-type and M259T Rubiscos were therefore co-transformed with plasmids directing the expression of GroES–GroEL, KJE (DnaK/DnaJ/GrpE) or TF. PAGE and carboxyarabinitol-binding analyses were performed on the total and soluble cellular *E. coli* proteins to confirm chaperone expression and measure the differences in Rubisco content and functional assembly (Figure 2). A comparison of the relative banding intensities in the total and soluble protein samples analysed by SDS/PAGE (Figures 2A and 2B respectively) showed the chaperones were highly expressed and soluble, while the majority of the abundant L subunit produced was prone to aggregation and was predominantly insoluble. Only the GroEL and its co-chaperonin GroES stimulated assembly of the M259T and wild-type PCC6301 Rubisco in *E. coli*.

Differences in the amount of soluble L subunit produced in the *E. coli* BL21(DE3) cells after 5 h of induction with IPTG at 23 °C (compared with 16 h in Figure 1) were confirmed by immunoblot analysis (Figure 2C) and correlated with the amount of L₈S₈ enzyme measured by [¹⁴C]-carboxyarabinitol-P₂ binding (Figure 2D), and non-denaturing PAGE (Figures 2E and 2F). Without additional GroES–GroEL the amount of functional M259T Rubisco produced was approx. 9-fold that of the wild-type. Overexpression of GroES–GroEL enhanced the yield of functional wild-type Rubisco by approx. 9-fold, whereas the excess chaperonins evinced only a 30 % improvement in the amount of assembled M259T enzyme. In contrast, overexpression of

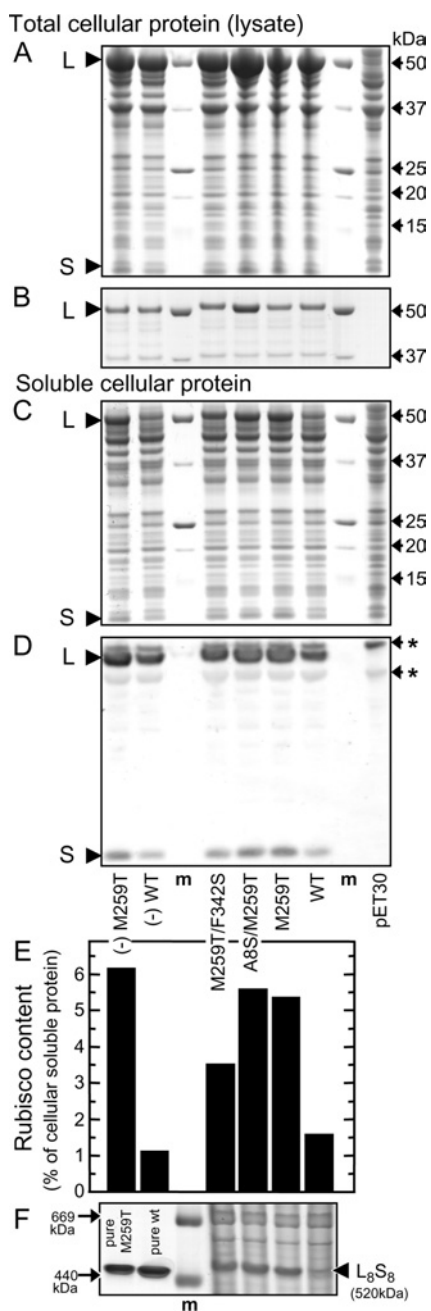


Figure 1 Evolved Rubisco variants fold and assemble more efficiently in *E. coli*

Rubisco expression was induced with IPTG in BL21(DE3) *E. coli* cells transformed with *rbcLS*-pET30a+ plasmids coding for wild-type (WT) and the evolved *Synechococcus* PCC6301 Rubisco variants (see Table 1). To compare the amount and partitioning of Rubisco L (52 kDa) and S (13 kDa) subunits in the soluble and insoluble protein cellular fractions, comparable samples of total cellular protein (lysate) containing 10 μ g (A) and 0.1 μ g (B) or only the soluble cellular protein fraction (10 μ g) (C) were separated by SDS/PAGE and visualized with Coomassie Blue staining. (D) Detection of the L and S subunit expression levels in the soluble cellular protein by immunoblotting using antibodies against *Synechococcus* sp PCC7942 Rubisco. (E) The amount of functional Rubisco measured by [14 C]carboxyarabinitol-P₂ binding, expressed as a percentage of the soluble cellular protein assuming a molecular mass of 65 kDa for each L subunit active site (assuming one S subunit for each L subunit that binds the [14 C]carboxyarabinitol-P₂). (F) Coomassie Blue staining of soluble cellular protein (30 μ g) and purified L₈S₈ Rubisco separated by non-denaturing PAGE. m, molecular mass marker (sizes shown: 669 kDa, thyroglobulin and 440 kDa, ferritin); *, non-Rubisco *E. coli* proteins recognized by the antibody.

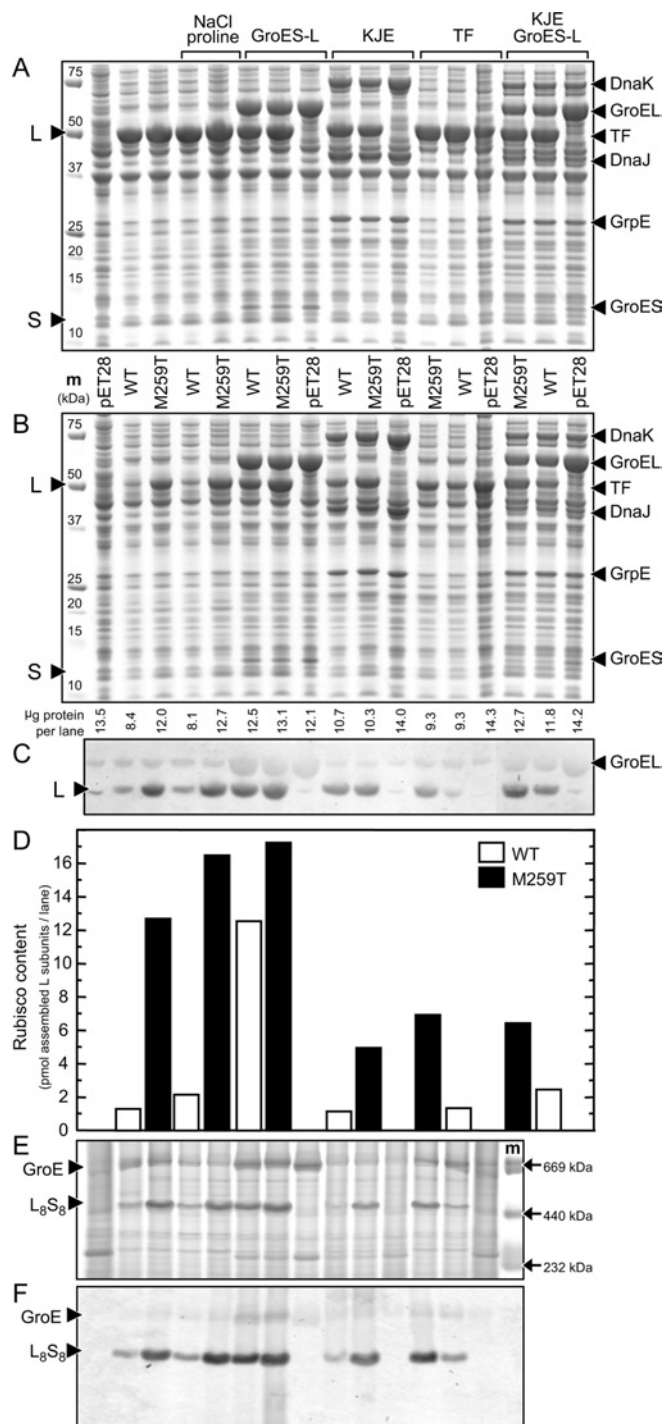


Figure 2 Influence of osmolites and *E. coli* chaperones on the expression and assembly of wild-type (WT) and the M259T *Synechococcus* PCC6301 Rubisco variants in BL21(DE3) *E. coli*

Total (A) and soluble (B) cellular protein from 1.5×10^6 cells separated by SDS/PAGE and visualized by Coomassie Blue staining. The relative amount of soluble protein loaded per lane is shown. (C) Detection of the L subunit in the soluble cellular protein by immunoblotting using an antibody against tobacco Rubisco that also recognizes the GroEL chaperonin and an unknown 50 kDa *E. coli* protein. (D) The amount of L subunit assembled into functional Rubisco measured by [14 C]carboxyarabinitol-P₂ binding. Soluble protein [twice that loaded in (B)] separated by non-denaturing PAGE, and the position of correctly assembled L₈S₈ Rubisco and the GroES–GroEL chaperonin complex (GroE) identified by Coomassie Blue staining (E) and immunodetection (F) with the tobacco Rubisco antibody. m, molecular mass markers (sizes shown). GroE–L, GroES (10.4 kDa) and GroEL (57.3 kDa) chaperonins; KJE, DnaK (70 kDa)–DnaJ (41 kDa)–GrpE (22 kDa) chaperones; TF, trigger factor (50 kDa).

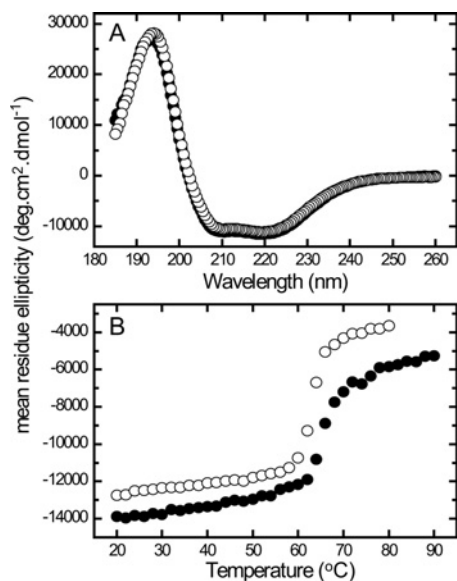


Figure 3 Unfolding of the M259T and wild-type Rubiscos

(A) CD spectra of equimolar amounts (0.31 μM) of His₆-tagged wild-type (WT) (●) and M259T (○) Rubisco are indistinguishable in the far-UV region indicating equivalent structural folding. (B) Thermally induced unfolding transitions of the Rubiscos monitored by CD at 222 nm.

the KJE and TF molecular chaperones reduced the amount of soluble wild-type and M259T L subunits produced (and accordingly the amount of L₈S₈ enzyme) by 20% and 40–60% respectively, indicating that incompatibilities between these chaperones and the L subunits hampered their productive folding (Figures 2C–2F). The overexpression of GroES–GroEL and KJE effected modest improvements of 30% and 70% in the amount of functional M259T and wild-type Rubisco produced respectively (Figure 2); no stimulation in functional Rubisco production by GroES–GroEL was evident in cells producing excess TF (results not shown). This suggests that under elevated levels of KJE and TF, assembly of L₈S₈ enzyme is limited primarily by the co-translational processing of both the wild-type and mutated *Synechococcus* L subunits.

Osmolite-assisted folding

Addition of the osmolite, proline, to the growth medium suppressed self-aggregation of the L subunits within *E. coli*. High concentrations of salt cause *E. coli* cells to concentrate proline *in vivo* and decrease the propensity of some proteins to aggregate [34]. In cells grown in LB supplemented with 20 mM proline and 300 mM NaCl, the solubility of both aggregation-prone L subunits for wild-type and M259T Rubiscos were both enhanced by 35% (Figure 2). The amount of additional soluble M259T L subunit exceeded the amount of extra wild-type soluble L subunit by a factor of approx. 5, indicating that aggregation of the mutant L subunit is more readily suppressed by proline.

In vitro thermostability and solubility

The structural integrity of the wild-type and M259T Rubiscos were compared by CD spectroscopy. Both enzymes showed matching CD spectra, indicating that their secondary structures were identical (Figure 3A). Thermally induced unfolding of the enzymes was also monitored by CD at 222 nm (Figure 3B). At this wavelength the melting temperature (T_M) for M259T Rubisco

($T_M = 63.5^\circ\text{C}$) was slightly lower than the wild-type enzyme ($T_M = 65^\circ\text{C}$), suggesting that the M259T mutation may slightly compromise the structural integrity of the L₈S₈ complex. Using the same enzyme preparations, no intrinsic improvement in the solubility of the M259T Rubisco relative to wild-type was evident by ammonium sulfate precipitation analyses (results not shown).

DISCUSSION

The expression of the *prkA* gene by *E. coli* is detrimental to cell viability because the bacterium does not ordinarily metabolize its catalytic product, ribulose-P₂ [35]. In the present study, we demonstrated that the adaptive M259T mutation overcame ribulose-P₂ toxicity during selection by increasing the pool of correctly folded Rubisco molecules. To our knowledge, this is the first reported mutation that confers an improvement to productive Rubisco assembly within *E. coli*.

Our results suggest that the M259T mutation may improve the capacity for productive folding of the L subunits by either reducing their propensity to form kinetically trapped misfolded intermediates and/or by improving their post translational processing by GroES–GroEL chaperonins. The increased assembly of the M259T L₈S₈ holoenzyme (relative to the wild-type control) in cells treated with the osmolite proline (Figure 2) confirmed that the mutant L subunits were less prone to unproductive aggregation. Overexpression of both the TF and KJE chaperones clearly constrained productive assembly of both wild-type and M259T Rubiscos, and this limitation was not overcome by the overproduction of GroES–GroEL. This implies there are incompatibilities between the L subunits and the co-translational activities of the TF and the KJE chaperone machinery, resulting in an increased susceptibility of the L subunit to form misfolded intermediates. However, at normal physiological levels of TF and KJE excess levels of GroES–GroEL enhance wild-type L₈S₈ production 9-fold, indicating under these physiological conditions productive folding of L subunits was limited by post-translational processing by the GroES–GroEL chaperonin complex, which is consistent with previous observations [14,32]. Similar yields of the M259T Rubisco were obtained at normal physiological chaperone levels. This implies the post-translational assembly limitation seen for wild-type L subunit is not as severe for the mutated L subunit, suggesting the M259T mutation improves productive interaction between the L subunit and the GroES–GroEL chaperonin complex. Under saturating levels of GroES–GroEL, the marginal improvements in M259T Rubisco production (0.3-fold yield increase; Figure 2) suggests productive folding of the M259T L subunits become limited prior to their transfer to GroEL, possibly stemming from incompatibilities with the TF and KJE chaperone machineries.

The propensity for the *Synechococcus* PCC6301 L subunits to misfold and aggregate in *E. coli* indicates that its chaperones (particularly TF and KJE [27,33]) have not been optimized for this protein. These incompatibility problems suggest that wild-type Rubisco assembly might be improved by the transplantation of the analogous chaperone genes from *Synechococcus* PCC6301 into *E. coli* or by directed evolution of the *E. coli* chaperones towards optimum L₈S₈ assembly. A limitation to both strategies is the possibility that the folding and assembly of native *E. coli* proteins may be unfavourably impaired, as observed previously when increasing GFP (green fluorescent protein) expression in *E. coli* through directed evolution of GroES–GroEL [36].

Previous amino acid replacements in Rubiscos, introduced through site-directed or random mutagenesis, have sometimes conferred improvement in one or more catalytic properties, but

always to the detriment of another [1,6,29,37]. Such catalytic trade-offs are apparently commonplace for Rubiscos in both natural and artificial selection. However, the M259T Rubisco characterized here is novel in that the improvements in k^c_{cat} and K_M for CO₂ occurred with little, or no, detriment to its specificity ($S_{c/o}$) or its K_M for ribulose-P₂ (Table 2). Notably, the 12 % improvement in k^c_{cat} for the M259T Rubisco contrasts with the 5-fold difference in specific activity measured previously for purified His₆-tagged wild-type and M259T Rubisco [16]. Previous mutagenic studies have highlighted that subtle modifications to the length and amino acid composition of the *Synechococcus* Rubisco L subunit C-terminus significantly perturbs the kinetics of the enzyme [17,28,29]. The extent to which the C-terminally appended GHHHHHH sequence affected the kinetics of the wild-type and M259T Rubiscos relative to each other and the native (non-tagged) enzymes was not examined.

Curiously Met²⁵⁹ is positioned close to the surface of the protein, within the solvent channel that traverses the hexadecamer along its fourfold axis (see Supplementary Figure 1 at <http://www.BiochemJ.org/bj/404/bj4040517add.htm>). At this position Met²⁵⁹ does not interact closely with any active site residues or with residues from other subunits in the L₈S₈ complex. Other mutagenic studies on form I Rubiscos, particularly those targeting modifications to residues at the L and S subunit interface, have also shown that perturbations to residues distant from the active site have significant influences on the kinetic properties of enzyme [6,37]. The changes in enzyme kinetics are caused by subtle changes to the active site geometry, and/or changes in the conformational dynamics of the L₈S₈ holoenzyme (either in mobile structural elements such as loop 6 [1,4,38] or in larger scale conformational changes [39]). Curiously the same M259T mutation has been selected previously using a *trans*-complementation screen of an XL1-Red generated *Synechococcus* PCC6301 Rubisco mutant library using a Rubisco deficient strain of the bacterium *Rhodobacter capsulatus* [40]. Notably the expression level, and kinetics, of the selected M259T variant in *R. capsulatus* were not quantified and therefore it remains to be assessed whether, as in *E. coli*, the M259T Rubisco supported growth of the mutated bacterium due to its improved tendency toward productive assembly.

Modest changes were observed in the kinetic properties of the two other Rubisco variants selected in *E. coli*, both of which shared the M259T mutation. The additional mutations in the A8S/M259T and M259T/F342S enzymes resulted in further improvements in their K_c and K_{RuBP} , with slight reductions in $S_{c/o}$ and k^c_{cat} (compared with the parental M259T enzyme; Table 2). Like the M259T mutation, it is not readily evident from the positioning of both these amino acids in the *Synechococcus* Rubisco crystal structure how they impart the changes in kinetics. Ala⁸ is within the highly divergent N-terminal region of the L subunit exposed to the external solvent that, in the crystal structure, resides at the interface between an L and an S subunit (see Supplementary Figure 1). Despite the high variability at the N-termini between different L subunits, this region has a significant influence on the catalytic prowess of both plant and bacterial Rubiscos (see [29] for a summary). Phe³⁴² is more highly conserved, presumably due to its close location downstream of the highly conserved loop 6 region (Gly³²⁶–Gly³³⁴ in PCC6301, which corresponds to residues 329–337 in the spinach L subunit), which plays an integral part during catalysis [1]. When compared with other cyanobacteria L subunit sequences (see below) only the aromatic phenylalanine and tyrosine amino acids are found at the equivalent position to codon 342. Again, two other Phe³²⁴ mutants were identified in the aforementioned *R. capsulatus*-based selection of *Synechococcus* Rubisco; the kinetics of the F324V, but not the F324I, enzyme

were characterized [40]. Comparable to that measured here for the M259T/F342S Rubisco, the K_{RuBP} for the F342V enzyme was reduced by approx. 50 %, the k^c_{cat} was approx. 30 % lower and the $S_{c/o}$ marginally compromised. However, in contrast to the 24 % decrease in K_c for the M259T/F342S Rubisco the K_c was approx. 50 % higher for the F342V enzyme. Since the individual A8S and F342S substitutions did not emerge in the selection, we did not examine their effects upon the kinetic properties of *Synechococcus* PCC6301 Rubisco.

Alignment of other cyanobacterial L subunits shows that many natural homologues possess a threonine residue at position 259. The catalytic improvement in the *Synechococcus* PCC6301 Rubisco imparted by the M259T mutation raises the question: why wasn't Thr²⁵⁹ fixed in Nature? Comparison of 21 different cyanobacterial genomes available from the JGI (Joint Genome Institute) and NCBI (National Center for Biotechnology Information) databases found four species contained threonine, five glutamine and the remainder methionine residues at the position equivalent to codon 259 (see Supplementary Figure 2 at <http://www.BiochemJ.org/bj/404/bj4040517add.htm>). The kinetic improvements associated with the M259T mutation might not be sufficient to warrant selection of the M259T Rubisco in Nature. Alternatively, the mutation, although kinetically better, may be unfavourable in other ways, such as reducing the compatibility of the L subunit with cyanobacterial chaperone complexes or other interacting proteins, such as those involved in carboxysome formation. Clearly, future studies will have to evaluate the extent to which Rubiscos evolved in *E. coli* affect the fitness of their native hosts. The construction of a *Synechococcus* PCC6301 Rubisco mutant, similar to *Synechocystis* PCC6803 Syn6803Δrbc mutant [41], would enable such substitution studies.

Using transition-biased whole-gene mutagenesis, we have shown that the directed evolution of *Synechococcus* PCC6301 Rubisco in *E. coli* can lead to improvements in its biophysical and kinetic parameters. As indicated previously [16], selection for further kinetic improvements should be possible using Rubisco libraries constructed by more sophisticated mutagenic techniques. Modification of the selection process to favour the selection of mutants with improvements in other kinetic traits, such as its specificity for CO₂ over O₂ may also be possible. Importantly, the *E. coli*-based Rubisco selection may allow us to explore alternative sequence space not accessible to photosynthetic organisms whose survival is dictated by contingent physiological constraints.

We thank Ms Harley Jenks (Emory University) for assistance with reverse transcriptase–real time PCR, Dr Monica Gerth (Emory University) for help with CD, Dr Heather Kane (ANU Molecular Plant Physiology) for her help with the CO₂/O₂ specificity assays, Ms Emily Beck (ANU Molecular Plant Physiology) for access to her Rubisco alignment database and Dr Lisa Gloss (Washington State University) for helpful suggestions. This research was supported by NIH (National Institutes of Health)/NIAID (National Institute of Allergy and Infectious Diseases) (1 R21AI054602-01) and NIH/NIGMS (National Institute of General Medical Sciences) (1 R01 GM074264-01) grants awarded to D.G. and I.M.M. and by a Discovery grant (DP0450564) awarded to S.N.W. by the Australian Research Council.

REFERENCES

- 1 Parry, M. A., Andralojc, P. J., Mitchell, R. A., Madgwick, P. J. and Keys, A. J. (2003) Manipulation of Rubisco: the amount, activity, function and regulation. *J. Exp. Bot.* **54**, 1321–1333
- 2 Morell, M. K., Paul, K., Kane, H. J. and Andrews, T. J. (1992) Rubisco: maladapted or misunderstood?. *Aust. J. Bot.* **40**, 431–441
- 3 Wingler, A., Lea, P. J., Quick, W. P. and Leegood, R. C. (2000) Photorespiration: metabolic pathways and their role in stress protection. *Phil. Trans. R. Soc. Lond.* **355**, 1517–1529
- 4 Tcherkez, G. G. B., Farquhar, G. D. and Andrews, T. J. (2006) Despite slow catalysis and confused substrate specificity, all ribulose biphosphate carboxylases may be nearly perfectly optimized. *Proc. Natl. Acad. Sci. U.S.A.* **103**, 7246–7251

- 5 Jordan, D. B. and Ogren, W. L. (1981) Species variation in the specificity of ribulose biphosphate carboxylase/oxygenase. *Nature* **291**, 513–515
- 6 Spreitzer, R. J. and Salvucci, M. E. (2002) Rubisco: structure, regulatory interactions, and possibilities for a better enzyme. *Ann. Rev. Plant Biol.* **53**, 449–475
- 7 Andrews, T. J. and Whitney, S. M. (2003) Manipulating ribulose biphosphate carboxylase/oxygenase in the chloroplasts of higher plants. *Arch. Biochem. Biophys.* **414**, 159–169
- 8 Koonin, E. V. (2003) Horizontal gene transfer: the path to maturity. *Mol. Microbiol.* **50**, 725–727
- 9 Kurland, C. G., Canback, B. and Berg, O. G. (2003) Horizontal gene transfer: A critical view. *Proc. Natl. Acad. Sci. U.S.A.* **100**, 9658–9662
- 10 Delwiche, C. F. and Palmer, J. D. (1996) Rampant horizontal transfer and duplication of rubisco genes in eubacteria and plastids. *Mol. Biol. Evol.* **13**, 873–882
- 11 Thomas, C. M. and Nielsen, K. M. (2005) Mechanisms of, and barriers to, horizontal gene transfer between bacteria. *Nat. Rev. Microbiol.* **3**, 711–721
- 12 Kimura, M. (1983) *The Neutral Theory of Molecular Evolution*. Cambridge University Press, Cambridge
- 13 Thornton, J. W. (2004) Resurrecting ancient genes: experimental analysis of extinct molecules. *Nat. Rev. Genet.* **5**, 366–375
- 14 Goloubinoff, P., Gatenby, A. A. and Lorimer, G. H. (1989) GroE heat-shock proteins promote assembly of foreign prokaryotic ribulose biphosphate carboxylase oligomers in *Escherichia coli*. *Nature* **337**, 44–47
- 15 Checa, S. K. and Viale, A. M. (1997) The 70-kDa heat-shock protein/DnaK chaperone system is required for the productive folding of ribulose-biphosphate carboxylase subunits in *Escherichia coli*. *Eur. J. Biochem.* **248**, 848–855
- 16 Parikh, M. R., Greene, D. N., Woods, K. K. and Matsumura, I. (2006) Directed evolution of Rubisco hypermorphs through genetic selection in engineered *E. coli*. *Prot. Eng. Des. Sel.* **19**, 113–119
- 17 Whitney, S. M. and Sharwood, R. E. (2007) Linked Rubisco subunits can assemble into functional oligomers without impeding catalytic performance. *J. Biol. Chem.* **282**, 3809–3818
- 18 Kane, H. J., Wilkin, J. M., Portis, A. R. and Andrews, T. J. (1998) Potent inhibition of ribulose-biphosphate carboxylase by an oxidized impurity in ribulose-1,5-biphosphate. *Plant Physiol.* **117**, 1059–1069
- 19 Pierce, J., Tolbert, N. E. and Barker, R. (1980) Interaction of ribulosebiphosphate carboxylase/oxygenase with transition-state analogues. *Biochemistry* **19**, 934–942
- 20 Schloss, J. V. (1988) Comparative affinities of the epimeric reaction-intermediate analogs 2- and 4-carboxy-D-arabinitol 1,5-biphosphate for spinach ribulose 1,5-biphosphate carboxylase. *J. Biol. Chem.* **263**, 4145–4150
- 21 Ruuska, S., Andrews, T. J., Badger, M. R., Hudson, G. S., Laisk, A., Price, G. D. and von Caemmerer, S. (1998) The interplay between limiting processes in C3 photosynthesis studied by rapid-response gas exchange using transgenic tobacco impaired in photosynthesis. *Aust. J. Plant Physiol.* **25**, 859–870
- 22 Morell, M. K., Paul, K., O'Shea, N. J., Kane, H. J. and Andrews, T. J. (1994) Mutations of an active site threonyl residue promote β elimination and other side reactions of the enediol intermediate of the ribulosebiphosphate carboxylase reaction. *J. Biol. Chem.* **269**, 8091–8098
- 23 Andrews, T. J. (1988) Catalysis by cyanobacterial ribulose-biphosphate carboxylase large subunits in the complete absence of small subunits. *J. Biol. Chem.* **263**, 12213–12219
- 24 Kane, H. J., Viil, J., Entsch, B., Paul, K., Morell, M. K. and Andrews, T. J. (1994) An improved method for measuring the CO₂/O₂ specificity of ribulosebiphosphate carboxylase-oxygenase. *Aust. J. Plant Physiol.* **21**, 449–461
- 25 Matsumura, I. and Ellington, A. D. (2001) *In vitro* evolution of β -glucuronidase into a β -galactosidase proceeds through non-specific intermediates. *J. Mol. Biol.* **305**, 331–339
- 26 Nishihara, K., Kanemori, M., Kitagawa, M., Yanagi, H. and Yura, T. (1998) Chaperone coexpression plasmids: differential and synergistic roles of DnaK–DnaJ–GrpE and GroEL–GroES in assisting folding of an allergen of Japanese cedar pollen, Cryj2, in *Escherichia coli*. *Appl. Environ. Microbiol.* **64**, 1694–1699
- 27 Nishihara, K., Kanemori, M., Yanagi, H. and Yura, T. (2000) Overexpression of trigger factor prevents aggregation of recombinant proteins in *Escherichia coli*. *Appl. Environ. Microbiol.* **66**, 884–889
- 28 Gutteridge, S. (1986) Mutagenesis and expression of cloned Rubisco (ribulose-biphosphate carboxylase). *Bioch. Soc. Trans.* **14**, 28–29
- 29 Kelllogg, E. A. and Juliano, N. D. (1997) The structure and function of Rubisco and their implications for systematic studies. *Am. J. Bot.* **84**, 413–428
- 30 Emlyn-Jones, D., Woodger, F. J., Price, G. D. and Whitney, S. M. (2006) RbcX can function as a Rubisco chaperonin, but is non-essential in *Synechococcus* PCC7942. *Plant Cell. Physiol.* **47**, 1630–1640
- 31 Andrews, T. J. and Ballment, B. (1984) A rapid, sensitive method for quantitating subunits in purified ribulose biphosphate carboxylase preparations. *Plant Physiol.* **75**, 508–510
- 32 Larimer, F. W. and Soper, T. S. (1993) Overproduction of *Anabaena* 7120 ribulose-biphosphate carboxylase/oxygenase in *Escherichia coli*. *Gene* **126**, 85–92
- 33 Kaiser, C. M., Chang, H.-C., Agashe, V. R., Lakshmiathy, S. K., Etchells, S. A., Hayer-Hartl, M., Hartl, F. U. and Barral, J. M. (2006) Real-time observation of trigger factor function on translating ribosomes. *Nature* **444**, 455–460
- 34 Ignatova, Z. and Gierasch, L. M. (2006) Inhibition of protein aggregation *in vitro* and *in vivo* by a natural osmoprotectant. *Proc. Natl. Acad. Sci. U.S.A.* **103**, 13357–13361
- 35 Hudson, G. S., Morell, M. K., Arvidsson, Y. B. C. and Andrews, T. J. (1992) Synthesis of spinach phosphoribulokinase and ribulose 1, 5-biphosphate in *Escherichia coli*. *Aust. J. Plant Physiol.* **19**, 213–221
- 36 Wang, J. D., Herman, C., Tipton, K. A., Gross, C. A. and Weissman, J. S. (2002) Directed evolution of substrate-optimized GroEL/S chaperonins. **111**, 1027–1039
- 37 Spreitzer, R. J., Peddi, S. R. and Satagopan, S. (2005) Phylogenetic engineering at an interface between large and small subunits imparts land-plant kinetic properties to algal Rubisco. *Proc. Natl. Acad. Sci. U.S.A.* **102**, 17225–17230
- 38 Cleland, W. W., Andrews, T. J., Gutteridge, S., Hartman, F. C. and Lorimer, G. H. (1998) Mechanism of Rubisco: the carbamate as general base. *Chem. Rev.* **98**, 549–562
- 39 Schlitter, J. and Wildner, G. F. (2000) The kinetics of conformation change as determinant of Rubisco's specificity. *Photosynth. Res.* **65**, 7–13
- 40 Smith, S. A. and Tabita, F. R. (2003) Positive and negative selection of mutant forms of prokaryotic (cyanobacterial) ribulose-1,5-biphosphate carboxylase/oxygenase. *J. Mol. Biol.* **331**, 557–569
- 41 Amichay, D., Levitz, R. and Gurevitz, M. (1993) Construction of a *Synechocystis* PCC6803 mutant suitable for the study of variant hexadecameric ribulose biphosphate carboxylase/oxygenase enzymes. *Plant Mol. Biol.* **23**, 465–476

Received 11 January 2007/12 March 2007; accepted 21 March 2007

Published as BJ Immediate Publication 21 March 2007, doi:10.1042/BJ20070071